British Journal of Healthcare and Medical Research - Vol. 12, No. 01
Publication Date: February 25, 2025
DOI:10.14738/bjhr.1201.18268.
Ramirez, A., Corro, G., & Flores, E. M. (2025). Dielectro Phoretic Force Spectroscopy in Short Blood Cell Aggregations. British Journal of Healthcare and Medical Research, Vol - 12(01). 393-405.

Dielectro Phoretic Force Spectroscopy in Short Blood Cell Aggregations

Araceli Ramirez
Centro de Nanotecnología,
Benemérita Universidad Autónoma de Puebla, Pueblar, Mexico

Griselda Corro
Facultad de ingeniería química,
Benemérita Universidad Autónoma de Puebla, Puebla, Mexico

Esteban Molina Flores
Centro de Nanotecnología,
Benemérita Universidad Autónoma de Puebla, Pueblar, Mexico

ABSTRACT

Aggregation of red blood cells and specifically linear rouleau formation of human erythrocytes affects the rheology of blood microcirculation and is widely under study to quantify flow abnormality in pathological conditions. Dielectric properties of cell suspensions or of undiluted whole blood are strongly related to the geometrical structure of particles. Electrophoretic measurements of rouleaux, formed through side-by-side adhesion of a small or even considerable number of erythrocytes, in suspending media of different electrical conductivity have the potential of size characterization and spatial separation of cell subpopulations due to their different polarizabilities. In the present paper we show that the electrophoretic force on red blood cell aggregations of different sizes, exposed to an electric field of variable frequency, and given correct medium permittivity and conductivity, provides a means for spatial separation and sorting of rouleaux with different 'stack number' of aggregated erythrocytes. In dependence on this number, i.e. on different but discrete measures of rouleau lengths, the dielectrophoretic force is calculated and represented against the frequency of the applied a.c. field. Predictions of frequency regions in the range of 10 to 100 MHz are made, where the amount and the direction of dielectrophoresis forces is different for different rouleau sizes. The field-flow-fractionation technique is a suitable tool, where the differential positioning of particles of definite size within a suspension flow velocity profile is established by the action of matching dielectrophoretic forces. Increased aggregation of red blood cells is considered an important factor in the development of vascular diseases and microcirculation impairment. The progressing diversity and size of rouleaux characterized by their 'stack number' might be a possible diagnose tool in the assessment of abnormal rheological properties.

Keywords: Erythrocytes, Rouleaux, Dielectrophoresis, Force effects, Sorting and separation.

INTRODUCTION

Dielectrophoresis (DEI)) is defined as the force acting on biological cells and colloidal particles in an inhomogeneous electric field. Specific physical and electrical properties of the particles and the suspended medium allow for their manipulation. By measuring the spectral impedance of individual cells as well as discriminating between cell types according to their dielectric properties, the technique is aimed at diagnostic applications for cell counting and separation in hematology, oncology or toxicology [1, 2, 3]. Recent activity reports include the sorting of biological samples such as bacteria [4], red blood cells [5, 6, 7] and DNA [8, 9]. Although DEP is effective for cell isolation, it is often coupled with other techniques, as e.g. Raman spectroscopy, to provide quantitative and qualitative information [10]. A review of the mathematical treatment of DEP is beyond the scope of this paper. However, several reviews have been published previously [10, 1 1, 12, 13].

The direction of movement of particles and the acting absolute force on them is bound to the knowledge of the internal electric field strength as a basic aspect of the study of many biological effects. The contour of the sample has a strong impact on it. Spherical and ellipsoidal cell models are frequently used due to the fact that linearly polarized electric plane waves generate a uniform local field distribution accessible by closed analytical solutions of the Laplace equation. However some biological cells, including erythrocyte rouleaux, deviate form the ellipsoidal form, and in order to account for these special shaped cells, more satisfactory cell models with shapes close to disks or cylinders [14] have been considered. Numerical methods commonly used for field characterization within a biological structure are based on Mie theory or the finite element (FE) and the finite difference time domain (FTD) techniques [15, 16]. Extensive computer calculations are required, though [17], and a simpler approach is desirable and often sufficient. The rouleau formation of erythrocytes, also quoted by its similarity as linear 'coin stacks' of several individual cells, translates into a cylindrical cell model. Characterized by an integer number of single cell heights, the aggregation of three or more cells would change the cell geometry in an ellipsoidal model from oblate to prolate. The local field and the induced dipole moment is thus affected considerably.

In this paper we show, that the multiplicity of erythrocyte cell aggregations can be followed up by dielectrophoresis, and a size-selective separation can be achieved, given suitable medium permittivity and conductivity, as well as frequency of the applied electric field. While the approximation of larger erythrocyte columns as general spherical ellipsoids is sufficient, an approximation procedure for dielectric bodies of short cylindrical shape is described and applied on stacks of erythrocytes with variable height-to-radius relation.

Dielectric Force

Dielectrophoretic forces are caused by the interaction of non-uniform electric fields with dielectric objects, which are suspended and free to move in a conductive medium. In inhomogeneous A.C. fields, the time averaged force < F > which is acting on a homogeneous dielectric particle, can be expressed by

$$< \vec{F} >= \frac{1}{2} \mathrm{Re}\left\{ \vec{m} \cdot \nabla \vec{E}^{*} \right\} \qquad (1)$$

where m is the induced dipole moment, $\nabla\vec{E}^*$ is the gradient of the complex conjugate of the external field, and Re denotes the real part of the scalar product. The induced dipole moment $\vec{m}$ is proportional to the particle volume V, the acting external electric field $E = E_0 \cdot e^{j\omega t}$ of circular frequency ω, and the permittivity $\varepsilon_0\varepsilon_m$ of the medium surrounding the dielectric object.

The time-averaged force acting on a homogeneous ellipsoidal particle is given by

$$< \vec{F}_{DEP} >= \varepsilon_0\varepsilon_m \cdot V \cdot \mathrm{Re}\{K(w)\} \nabla |E_{rms}|^2 \quad (2)$$

$$K(w)_x = \frac{\varepsilon_p^* - \varepsilon_m^*}{\varepsilon_m^* + (\varepsilon_p^* - \varepsilon_m^*) \cdot n_x} \quad (3)$$

with the component in x-direction of the Clausius-Mossotti factor. ε_P^* is the complex permittivity of the particle, and n_x is the Lorentz depolarization factor in x-direction parallel to the external field. The Clausius-Mossotti factor is a measure of the effective polarizability of the particle, and depends for nx strongly on the geometrical shape of the ellipsoidal object. With c the permittivity and c; the electrical conductivity of a dielectric medium, the complex permittivity is defined as $\varepsilon^* = \varepsilon - (\sigma / \varepsilon_0\omega)$ being j the imaginary unit $(-1)^{1/2}$. Consequently, the Clausius-Mossotti factor depends on the frequency of the applied field, besides the dielectric properties of particle and medium. When only frequency dependencies are the objective of the study, it is sufficient to consider $K(\omega)$ as the only frequency dependent part of the induced dipole moment. Variations of this factor give rise to the dielectrophoretic force described in (2), which is unique to a special particle type. This concerns not only intrinsic dielectric properties, but also the geometrical shape via the depolarization factors and the size via the volume contained in the induced dipole moment. These latter aspects will play a particular role in the present paper.

Shape and size variation of the particles affect $K(\omega)$ and V, which leads to readily achievable dielectrophoretic separation protocols. The design and geometry of the microelectrodes used to generate and control the non-uniform electric field is also an important factor to be considered. The force $< F_{DEP} >$ is toward the high electric field, and the particles collect at the electrode edges, if $\mathrm{Re}\{K(\omega)\} > 0$, on the contrary the force is in direction of the decreasing field, if $\mathrm{Re}\{K(\omega)\}$ is negative. From expression (3) follow two special cases of practical importance: at the one hand sphere-shaped particles with $n_x = n_y = n_z = 1/3$,yielding

$$< F_{DEP} >_{sphere} = 2\pi r^3 \varepsilon_0 \varepsilon_m^* \,\mathrm{Re}\left\{\frac{\varepsilon_p^* - \varepsilon_m^*}{\varepsilon_p^* + 2\varepsilon_m^*}\right\} \nabla |E|^2 \quad (4)$$

URL: http://dx.doi.org/10.14738/bjhr.1201.18268.

and at the other hand long cylinder-shaped particles with $n_x = 0, \left(n_y = n_z = 0.5\right)$

$$< F_{DEP} >_{needle} = \frac{\pi r^2 \ell}{3} \varepsilon_0 \varepsilon_m^* \operatorname{Re}\left\{\frac{\varepsilon_p^* - \varepsilon_m^*}{\varepsilon_p^* + 2\varepsilon_m^*}\right\} \nabla \left|E\right|^2 \tag{5}$$

where r is the radius of the cylinder and C its length. It is clear, that the applicability of expressions (4, 5) has to be verified with respect to the particle shape in any practical approach.

ERYTHROCYTE ROULEAUX DEFINED BY SHORT CYLINDERS

The calculation of force effects on biological cells starts commonly with a solution of the Laplace equation under quite restrictive conditions. In order to arrive at closed expressions, an ellipsoidal cell model with a confocal shell is commonly assumed, as only such geometry exhibits a constant local field. Normal human erythrocytes are nonnucleated biconcave disk-shaped cells of about 7.5 him in diameter with edges that are thicker than the center part. Indeed, they resemble an oblate ellipsoid only in a crude approach. The determination of the induced dipole moment for such a structure in field direction will be possible only to a certain approximation, e.g., of a very short circular cylinder (flat disk) of radius and half length with. Erythrocyte aggregation and the formation of linear rouleaux has been widely investigated and its importance in the rheology of blood circulation is well established [18, 19]. The size of such 'coin stacks' is of clinical relevance, stimulating interest for their analysis and manipulation.

The aggregation of disk-shaped objects to columns has a clear effect on the local field and the induced dipole moment. While the depolarization factor in direction of the rouleaux (cylinder) axis parallel to the external electric field takes a value close to 0 for leading to the expression (5), for a disk, this value is closer to 1. In linearly polarized A.C. fields, particles are oriented along their axis of highest polarization. A long cylinder will line up with its symmetry axis along the field, while a circular disk lines up along its radius. The orientation of a cube-like object (cylinder with) results in uncertainty.

It is important to remember, that the side-by-side aggregation of individual erythrocytes generates columns of length with the thickness of a single cell and a stack number. While single or double erythrocytes orient themselves with the radius as mayor axis along the external field, aggregations of more than three erythrocytes results in cylinder-shaped structures with. Depending on the number s, the axis ratio, the depolarization factor and the induced dipole moment change correspondingly, and so does the dielectrophoretic force acting on any of the rouleaux.

For the sake of simplicity, only electric effects are considered here, although hydrodynamic friction or motions induced by temperature fields are not without importance, particularly at elevated medium conductivities.

INDUCED POLARIZATION IN A CYLINDER-SHAPED DIELECTRIC BODY

In the Laplace model, a homogeneous ellipsoid possesses a constant local field. Integration over this field leads to the induced polarization and thus to expressions related to force actions on the special object. Already in such important cases as for a cube or a short cylinder is it difficult

to calculate the depolarization factors without accepting an ellipsoid as substituting shape of the object. But even then is the best shape of it to be used, and the next approximation step not a straightforward choice.

This chapter deals with an approximation procedure for the calculation of the internal local field $\overrightarrow{E_i}\left(\vec{r}\right)$ in a material body of general shape and a dielectric constant ε_p^*, which is brought into a given field $\overrightarrow{E_0}\left(\vec{r}\right)$, acting inside a suspending medium of dielectric permittivity ε_m^*.

The problem can be formulated as follows: The local field (P) causes a polarization $\vec{P} = \varepsilon_0(\varepsilon_p^* - \varepsilon_m^*)\overrightarrow{E_i}$. On an surface element $\Delta\vec{F}$ of the dielectric body, this polarization generates a polarization charge $\Delta q = \sigma_{pol} \cdot \Delta F = \overrightarrow{P} \cdot \Delta\vec{F}$, which by virtue of the Coulomb law, together with the unperturbed field $\overrightarrow{E_0}\left(\vec{r}\right)$, produces the local field such that

P

$$\overrightarrow{E_i}(\vec{r}_1) = \overrightarrow{E_0}(\vec{r}_1) - \iint \frac{\vec{r}_{12}}{4\pi\varepsilon_0 r_{12}^3}\left[\vec{P}(\vec{r}_2)\,\Delta\overrightarrow{F_2}\right]. \qquad (6)$$

The integration is carried out over the surface of the dielectric body; $\Delta\vec{F}$ points outward, and $\overrightarrow{r_{12}}$ combines the origin with the integration element at $\vec{r}_2$. The relation between $\overrightarrow{E_0}\left(\vec{r}\right)$ and $\overrightarrow{E_i}\left(\vec{r}\right)$ is supposed by us to be linear, thus

$$\vec{P}\left(\vec{r}\right) = \varepsilon_0(\varepsilon_p^* - \varepsilon_m^*)\overrightarrow{E_i}(\vec{r}) = \varepsilon_0(\varepsilon_p^* - \varepsilon_m^*)\overrightarrow{E_0}(\vec{r})\alpha(\vec{r}) \qquad (7)$$

In general, $\alpha\left(\vec{r}\right)$ is a tensor, as the directions of $\overrightarrow{E_i}$ and $\overrightarrow{E_0}$ are not necessarily parallel. It further depends on the place inside the sample due to the locally different action of the polarization charges.

In order to calculate $\vec{P}\left(\vec{r}\right)$ or $\vec{E}\left(\vec{r}\right)$ from expressions (6,7), we make the assumption, that 01 does not depend on $\vec{r}$. The polarization established inside the dielectric particle, is due to the displacement of electrical charges enforced by the field $\overrightarrow{E_0}\left(\vec{r}\right)$. Surface charges are built up (on S and C in Fig. 1b) and counteract the complete displacement corresponding to the field $\overrightarrow{E_0}\left(\vec{r}\right)$. We will suppose here, that the whole set of charges experiences the same displacement, which means, that (I constant. We further suppose, that the polarization vector $\vec{P}$ points more or less into the direction of $\overrightarrow{E_0}\left(\vec{r}\right)$, i.e., we will consider the projection of the field, generated by the polarization charges, on the direction of $\overrightarrow{E_0}\left(\vec{r}\right)$:

$$\vec{P}(\vec{r}_1) = \varepsilon_0(\varepsilon_p^* - \varepsilon_m^*)\alpha_1\overrightarrow{E_0}(\vec{r}_1)$$

URL: http://dx.doi.org/10.14738/bjhr.1201.18268.

$$= \varepsilon_0(\varepsilon_p^* - \varepsilon_m^*)\left\{\overrightarrow{E_0}(\vec{r_1}) - \iint \frac{(\varepsilon_p^* - \varepsilon_m^*)\alpha_1}{4\pi} \cdot \frac{\overrightarrow{E_0}(\vec{r_2})\,d\overrightarrow{F_2}}{r_{12}^3} \cdot \frac{\overrightarrow{E_0}(\vec{r_1})\overrightarrow{r_{12}}}{\overrightarrow{E_0}^2(\vec{r_1})} \cdot \overrightarrow{E_0}(\vec{r_1})\right\}$$

$$\alpha_1 = \left\{\varepsilon_m^* 1 + \frac{\varepsilon_p^* - \varepsilon_m^*}{4\pi} \iint \frac{\overrightarrow{E_0}(\vec{r_2})\,d\overrightarrow{F_2}}{r_{12}^3} \cdot \frac{\overrightarrow{E_0}(\vec{r_1})\overrightarrow{r_{12}}}{\overrightarrow{E_0}^2(\vec{r_1})}\right\}^{-1} \tag{8}$$

This value allows considering a first approximation of the polarization $\vec{P}_1$, which on the surface of the dielectric body generates charges, and thus an additional field inside the dielectric. The problem would be completely solved if the total field at any place fulfills already the condition $\overrightarrow{E_i} = \vec{P}_1 / \varepsilon_0(\varepsilon_p^* - \varepsilon_m^*)$, but in general, the polarization $\vec{P}_1$ of the first approximation step will not be sufficient to describe the real situation, and a field $\overrightarrow{E_1}(\vec{r})$ keeps acting on the dielectric with the effect of the additional polarization $\overrightarrow{P_2}(\vec{r})$,

$$\overrightarrow{E_1}(\vec{r}) = \overrightarrow{E_0}(\vec{r}) - \iint \frac{\overrightarrow{r_{12}}}{4\pi\varepsilon_0 r_{12}^3}\left(\overrightarrow{P_2}(\vec{r_2})\,d\overrightarrow{F_2} - \overrightarrow{P_1}(\vec{r_1}) / \varepsilon_0(\varepsilon_p^* - \varepsilon_m^*)\right) \tag{9}$$

$\overrightarrow{P_2}(\vec{r})$ can be calculated with $\overrightarrow{E_1}(\vec{r})$ in the same way, as $\vec{P_1}(\vec{r})$ was calculated with $\overrightarrow{E_0}(\vec{r})$. The number of approximation steps needed to achieve the best result depends on the complexity of the shape of the dielectric body, as well as on the allowed error of the result.

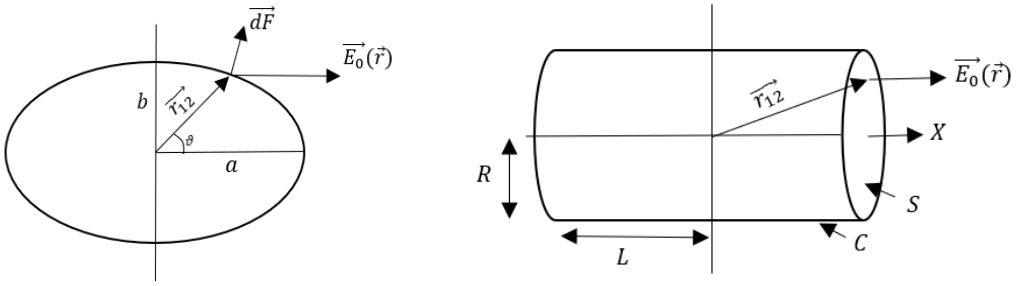

(a) **(b)**

Fig. 1: (a) Prolate ellipsoid with indication of used symbols in the calculus. (b) Dielectric cylinder of diameter 21? and length 21.

Exact solutions with a constant cc are known for the sphere, the infinitesimal thin wire (needle), and the infinitesimal extended disk (sheet). When our approach is applied here, already the first approximation step gives the exact solution, as it should, when $\alpha(\vec{r}) = \alpha_1 = \text{constant}$.

The polarization of a prolate spheroid (Fig. la) result with expression (7) and $q^2 = b^2/\left(a^2 - b^2\right)$ in

$$\alpha = \left\{\varepsilon_m + \left(\varepsilon_p^* - \varepsilon_m^*\right)q^2\left(1 + \frac{\sqrt{q^2+1}}{2}\cdot \ell n\frac{\sqrt{q^2+1}-1}{\sqrt{q^2+1}+1}\right)\right\}^{-1} \qquad (10)$$

-1

For an oblate ellipsoid one gets instead

$$\alpha = \left\{\varepsilon_m + (\varepsilon_p^* - \varepsilon_m^*)(q^2+1)\left(q\, arctan\frac{1}{a} - 1\right)\right\}^{-1} \qquad (11)$$

and consequently with $q \to \infty$ (or $a = b$) we have for the sphere-shaped dielectric $\alpha_1 = 3/\left(\varepsilon_p^* + 2\varepsilon_m^*\right)$ yielding the known expression for the polarization vector

$$\vec{P} = 3\varepsilon_0 \frac{\varepsilon_p^* - \varepsilon_m^*}{\varepsilon_p^* + 2\varepsilon_m^*}\cdot \vec{E_0}.$$

It is easy to recognize, that $K(\omega) = 3\left(\varepsilon_p^* - \varepsilon_m^*\right)/\left(\varepsilon_p^* + 2\varepsilon_m^*\right)$, the Clausius-Mossotti factor, is in accord with expressions (2,4). Not so straightforward is the situation in the case of a short cylinder-shaped body (Fig. 1 b), as e.g. rouleaux are.

We proceed:

$$\iint \frac{\vec{E_0}(\vec{r_2})\,d\vec{F_2}}{r_{12}^3}\cdot\frac{\vec{E_0}(\vec{r_1})\vec{r_{12}}}{\vec{E}_0^2\left(\vec{r_1}\right)} =$$

$$= 2\int_0^R \frac{2\pi a da\cdot L}{\left(a^2+L^2\right)^{3/2}} = \int_L^{\left(R^2+L^2\right)^{1/2}} \frac{rdr}{r^3}\cdot 4\pi L$$

$$= 4\pi\left[-\left(1+R^2/L^2\right)^{-1/2}\right]$$

$$P_1 = \frac{\varepsilon_0(\varepsilon_p^* - \varepsilon_m^*)\vec{E_0}}{\varepsilon_m^* + (\varepsilon_p^* - \varepsilon_m^*)\left(1-\left(1+R^2/L^2\right)^{-1/2}\right)}.$$

This is a homogeneous polarization and only the first approximation, which is good enough for long cylinders with $L >> R$ or for disks with $R >> L$. Without going into further details of the calculus, one gets for the polarization of a short cylinder in a second approximation

URL: http://dx.doi.org/10.14738/bjhr.1201.18268.

$$\vec{P} = \varepsilon_0(\varepsilon_p^* - \varepsilon_m^*)\overrightarrow{E_0}\left\{\varepsilon_m^* + (\varepsilon_p^* - \varepsilon_m^*)\left(1-\left(1+R^2/L^2\right)^{-1/2}\right)\right\}^{-1} * \tag{12}$$

$$*\left\{1+\frac{1/2-\left(1+R^2/L^2\right)^{-1/2}-(1/2)\left(1+8L^2/R^2\right)^{-1}+(1/2L)\left(R^2+2L^2\right)\cdot\left(R^2+4L^2\right)^{-1/2}-(1/2L)R}{(\varepsilon_p^*-\varepsilon_m^*)^{-1}+1-7/16\left(1+11R^2/56L^2\right)}\right\}.$$

With the application in expression (12) of real values for R and L, which correspond to a single erythrocyte and an aggregation to a 'coin stack' of, say, ten erythrocytes, i.e. $\{2R = 7.5\mu m; 2L = 2.2\mu m\}$ and $\{2R = 7.5\mu m; 2L = 22\mu m\}$, respectively, a change of about 5:1 in the induced polarization happens. This, of course, must have a notable effect on the dielectrophoretic force, acting on such cylindrical particles. Corresponding to the tendency, that dielectric bodies align its axis of maximum polarization with the external field, erythrocyte cell aggregations up to the stacking number $s = 3$ will orient the single cell radius vector parallel to the external field, while for $s \geq 4$ a reorientation occurs and the cylinder axis aligns with the field (see Fig. 2).

DIELECTROPHORETIC FREQUENCY SPECTRUM ON FORCE

The frequency response of the DEP force on linear arrangements of erythrocyte 'coin stacks' is governed by expressions (2, 12) and the corresponding Clausius-Mossotti factor, which is related to cc (expression 7) by

$$K(\omega) = \alpha \cdot (\varepsilon_p^* - \varepsilon_m^*). \tag{13}$$

In the limiting cases of a long cylinder (needle) and a sphere, with $\alpha = 1/\varepsilon_m^*$ and $\alpha = 3/(\varepsilon_p^* + \varepsilon_m^*)$, respectively, the relations (4,5) are of course reproduced. In the following calculus the rouleaux are approximated to solid homogeneous cylinders of length $2L = s \cdot d$ (Fig. 2) with a relative permittivity $\varepsilon_p = 50$ and conductivity $\sigma_p = 0.5S/m$ [10].

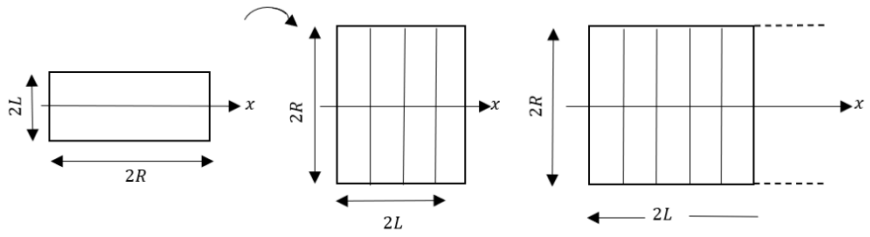

Fig. 2: Erythrocyte 'rouleaux '. Direction of maximum polarization is x. For s = l, 2, 3 the radius R of the cell aggregate aligns with the external field.

Using these parameters, a plot of the frequency variation of the polarization factor, estimated from expression (13) was calculated as a function of frequency and rouleaux-length parameter s at different aqueous medium conductivities between $0.001S/m$ *and* $0.1\ S/m$.

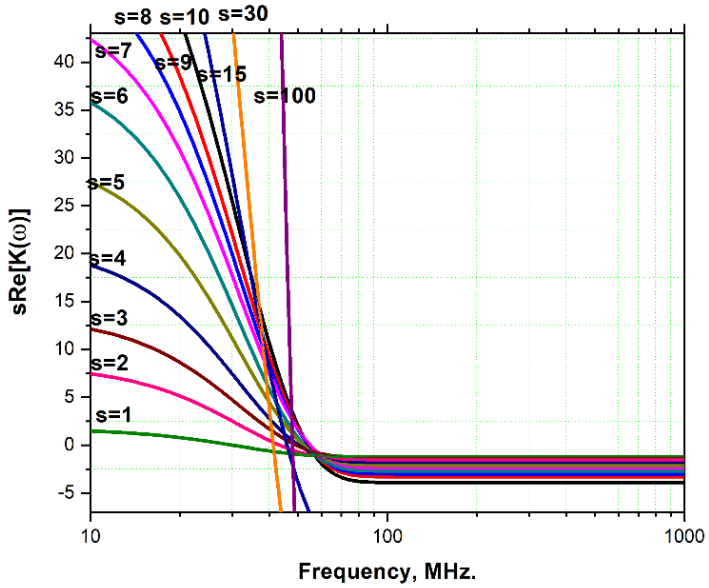

Fig. 3: Real part of the Clausius-Mossotti factor multiplied by the erythrocyte stack number s, measured against the A.C. electric field frequency. The stack number s is a rouleaux size parameter, meaning $s=1$ a single erythrocyte, and $s\geq 2$ a linear cell aggregation of two or more erythrocytes. The conductivity and relative permittivity of the internal cell and the suspending medium are taken as 0.5 $S\cdot m^{-1}$ and 0.01 $S\cdot m^{-1}$, as well as 50 and 80, respectively. Particle dimensions are $2R$ = $7.5\ \mu m$, with s 1, 2, 3 ,…, characterizing the linear side-by-side adhesion of erythrocytes. $s=100$ might not be a real situation, but represents the often applied border case of an 'infinite' cylinder length.

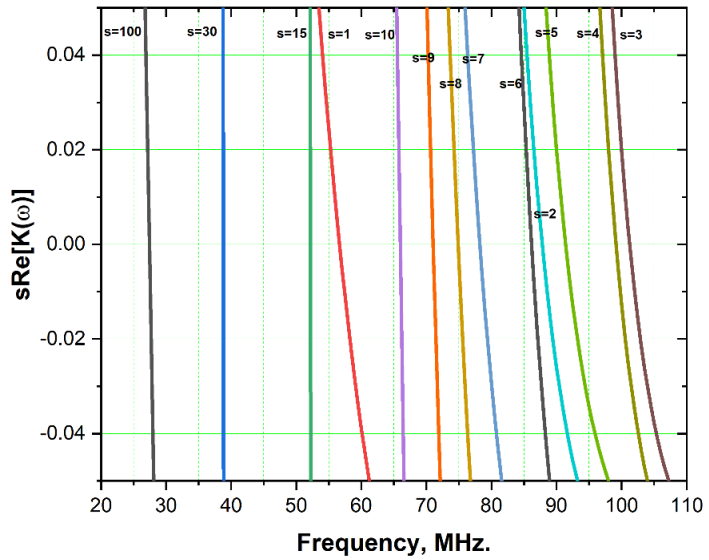

Fig. 4: Detail of the frequency region, where the dielectrophoretic force goes negative for cell aggregates of different size in a medium of conductivity $\sigma_m = 0.01\ S\cdot m^{-1}$. The similarity between curves belonging to low values of s is a consequence of similar axis relations R/L due to the reorientation of aggregations with the external field vector along the major axis.

URL: http://dx.doi.org/10.14738/bjhr.1201.18268.

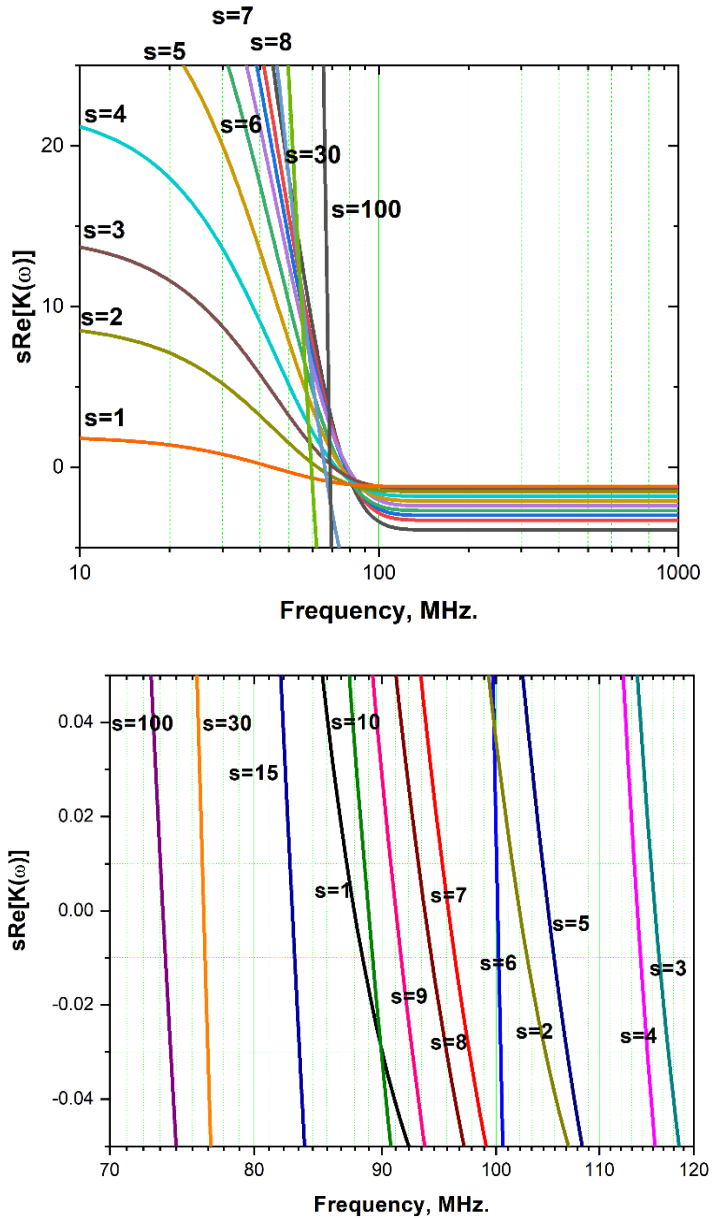

Fig. 5: Same as previous figures 3 and 4, but by a factor of 10 increased medium conductivity value of $\sigma_m = 0.1_{,} S \cdot m^{-1}$

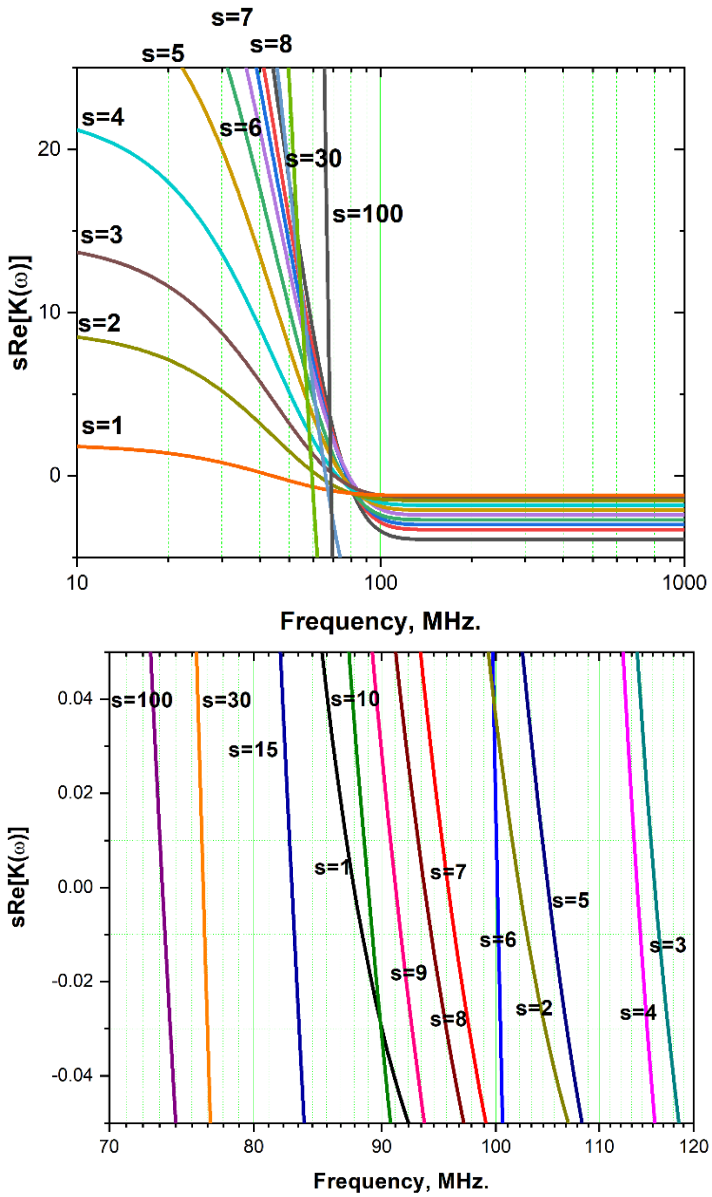

Fig. 5: Same as previous figures 3 and 4, but by a factor of 10 increased medium conductivity value of $\sigma_m = 0.1 . S \cdot m^{-1}$

The results for the dielectrophoretic force, which is proportional to s·Re[K(ω)], are shown in Figs. 3 through 5 for the case of σm=10mS/m and σm=100mS/m. As can be seen from this figures, the force on rouleaux of different length is indeed quite different, and in certain frequency ranges it remains positive for shorter cell aggregates, and goes negative at higher frequencies, while for long aggregates, this latter behavior is observed at lower frequencies. Although these figures do not show the absolute force on the rouleaux, it does represent the frequency variation and the direction of the force. As shown e.g. in Fig. 4 with more detail, the difference in the critical frequencies (defined by s·Re[K(ω)] =0) of rouleaux, formed of, say, 9 or 10 erythrocytes is about 4 MHz, which is easy to control under experimental conditions. For short rouleaux, the tendency to align the major particles axis with the external field leads to a reorientation process, if the cylinder half-length becomes smaller than the erythrocyte radius R (see Fig 2). This is the case for s=l,2,3, given that the outer erythrocyte thickness is more than

URL: http://dx.doi.org/10.14738/bjhr.1201.18268.

three times smaller than its diameter. It implies, that the induced dipole moment is similar for rouleaux with s=3&4, respectively. Nevertheless, is the DEP force at lower frequencies positive for all particle sizes and quite different in its amount, as indicated by the product of $s \cdot Re[K(\omega)]$ for a fixed frequency.

CONCLUSION

From previous figures it becomes clear that the DEP effect shows two regions of importance. The positive part means, that dielectric particles are attracted to the electrodes, contrary to the negative part, where the particles are rejected [20]. The cross-over frequency is the frequency in which the DEP force is equal to zero. It depends strongly on the conductivity and the permittivity of the particles and of the suspended medium. This is clearly seen in figs. 4 and 5, where the only changed parameter of the calculus is the medium conductivity of mS/m and σm=10mS/m and σm=100mS/m.

Known microelectrode arrays for batch and continuous separation of microorganisms and cells allow to achieve separation and sorting of a population of erythrocyte rouleaux. It is shown in this work that the induced dipole moment in erythrocyte rouleaux of different sizes of aggregation causes a dielectrophoretic force effect, which is different in magnitude for different rouleaux lengths. Additionally, do exist frequency windows, where this force is negative for one subpopulation, while it is positive for another one, providing for a means of sorting.

We have not included in our study the effect of size- and shape dependent friction, which the particles might suffer in its movement. The friction factor of a sphere, a disk, a cube or a cylinder depends in a complicated way on geometrical and hydrodynamic conditions of the rheological system. While for a sphere-like particle the friction factor is known to be proportional to the sphere radius R, other cases are not so straight forward. At any rate, the friction force counteracts and thus diminishes the DEP force on the considered particle.

Impedance spectroscopy enables rapid and convenient data acquisition; furthermore, it offers additional information since it is also phase sensitive.

References

1. Gascoyne PR, Shim S. "Isolation of circulating tumor cells by dielectrophoresis". Cancers (Basel). Mar 12;6(1);545-79. Epub 2014 Mar 12. 2014

2. Shim S, Stemke-Hale K, Noshari J, Becker FF, Gascoyne PR. "Dielectrophoresis has broad applicability to marker-free isolation of tumor cells from blood by microfluidic systems". Biomicrofluidics. (1);11808. Epub 2013 Jan 2013

3. Frusawa H. "Frequency-Modulated Wave Dielectrophoresis of Vesicles and Cells: Periodic U-Turns at the Crossover Frequency". Nanoscale Res Lett. 13(1):169. June 2018

4. Jones, P. V.; Huey, S.; Davis, P.; McLemore, R.; McLaren, A.; Hayes, M. A. "Biophysical separation of Staphylococcus epidermidis strains based on antibiotic resistance". Analyst 140, 5152—5161, 2015 doi:10.1039/C5AN00906E.

5. Qiang, Y.; Liu, J.; Mian, M.; Du, E. "Experimental electromechanics of red blood cells using dielectrophoresis-based microfluidics". In Mechanics of Biological Systems and Materials, Volume 6; Conference Proceedings

ofthe Societyfor Experimental Mechanics Series; Springer, Cham, 2017; pp. 129—134 ISBN 978-3319-41350-1.

6. Faraghat, S. A.; Hoettges, K. F.; Steinbach, M. K.; van der Veen, D. R.; Brackenbury, W. J.; Henslee, E. A.; Labeed, F. I-1.; Hughes, M. P. "High throughput, low-loss, low-cost, and label-free cell separation using electrophysiology-activated cell enrichment". Proc. Natl. Acad. Sci. U.S.A. 2017, 114, 4591-4596, doi:10.1073/pnas.1700773114.

7. Srivastava, S. K.; Daggolu, P. R.; Burgess, S. C.; Minerick, A. R. "Dielectrophoretic characterization of erythrocytes: Positive ABO blood types". Electrophoresis 29, 5033-5046, doi: 10.1002/elps.200800166. 2008

8. Jones, P. V.; Salmon, G. Ia.; Ros, A. "Continuous separation of DNA molecules by size using insulator-based dielectrophoresis". Anal. Chem. 89, 1531—1539, 2017 doi: 10.1021/acs.analchem.6b03369.

9. Song, Y.; Sonnenberg, A.; Heaney, Y.; Heller, M. J. "Device for dielectrophoretic separation and collection of nanoparticles and DNA under high conductance conditions: Nanoanalysis". Electrophoresis 36, 1107—1114, 2015 doi:10.1002/elps.201400507.

10. Hanson, Cynthia, "The Use of Microfluidics and Dielectrophoresis for Separation, Concentration, and Identification of Bacteria" All Graduate Theses and Dissertations. 7044. https://digitalcommons.usu.edu/etd/7044]. (2018)

11. [1 1] Jones, T. B. "Electromechanics of particles"; Cambridge University Press: Cambridge; New York, ISBN 9780-521-43196-5. 1995

12. [12]. Li, M.; Li, W. Fl.; Zhang, J.; Alici, G.; Wen, W. "A review of microfabrication techniques and dielectrophoretic microdevices for particle manipulation and separation". J. Phys. -Appl. Phys. 47, 063001, 2014, doi: 10.1088/00223727/47/6/063001.

13. Gagnon, Z. R. "Cellular dielectrophoresis: Applications to the characterization, manipulation, separation and patterning of cells". Electrophoresis 32, 2466— 2487, 2011, doi: 10.1002/elps.201100060.

14. J. L. Sebastián, S. Muñoz, M. Sancho, J. M. Miranda: "Analysis of the influence of the cell geometry, orientation and cell proximity effects on the electric field distribution from direct RF exposure", Phys. Med. Biol. 46, 213-225, 2001.

15. J. Stratton: Electromagnetic Theory (New York, McGraw-Hill) pp. 513-73 (1941).

16. P. Bernardi, M. Cavagnaro, L. M. d'lnzeo: "Cell modeling to evaluate EM field absorption in biological samples", URSIXXVI General Assembly, Canada, p.616 (1999).

17. T. B. Jones: Electromechanics ofparticles, Cambridge University Press, Cambridge (1995). [18] P. Foresto, M. D'Agrio, M. Carreras, RE, Cuezo, J. Valverde, R. Rasia: "Evaluation of red blood cell aggregations in diabetes by computerized image analysis", Medicina (B.Aires) 60, 570-572, 2000 [19] Qian C, Huang H, Chen L, Li X, Ge Z, Chen T, Yang Z, Sun L "Dielectrophoresis for bioparticle manipulation". Int J Mol Sci. Epub 2014 Oct 10. 2014

18. Yan Jun Kang, "Microfuidic based techniques for measuring RBC aggregation and blood viscosity in a continuous and simultaneous fashion", Micromechanics 9, 467, 2018 doi 10.3390/mi9090467, 2018

URL: http://dx.doi.org/10.14738/bjhr.1201.18268.